AIMS Mathematics, 10(10): 24712–24729.
DOI:10.3934/math.20251095
Received: 12 July 2025
Revised: 16 October 2025
Accepted: 21 October 2025
Published: 29 October 2025

https://www.aimspress.com/journal/Math

Research article

Analysis and simulation of a normalized Caputo-Fabrizio fractional SEIR epidemic model

Ramsha Shafqat[1,*], **Saeed M. Alamry**[2] **and Ateq Alsaadi**[2]

[1] Department of Mathematics and Statistics, The University of Lahore, Sargodha 40100, Pakistan
[2] Department of Mathematics and Statistics, College of Science, Taif University, P.O. Box 11099, Taif 21944, Saudi Arabia

* **Correspondence:** Email: ramshawarriach@gmail.com.

Abstract: This paper introduces, analyzes, and numerically investigates a fractional-order SEIR epidemic model employing the normalized Caputo-Fabrizio (NCF) derivative. The model captures memory effects and the role of an exposed (latent) compartment, allowing for more realistic epidemic dynamics. We establish existence, uniqueness, positivity, and population conservation, then propose a robust numerical scheme. The impact of the memory parameter and kernel normalization is illustrated via simulations, with a discussion on their significance for epidemic forecasting and potential real-world applications.

Keywords: fractional differential equation; normalized Caputo-Fabrizio; SEIR model; numerical outcomes
Mathematics Subject Classification: 34D20, 34K20, 34K60, 92C60, 92D45

1. Introduction

Mathematical modeling plays a vital role in understanding, forecasting, and controlling the spread of infectious diseases [1, 2]. Among the available approaches, compartmental models, such as the susceptible-exposed-infectious-recovered (SEIR) system, are widely regarded as essential for describing the fundamental mechanisms driving epidemic dynamics. These models are beneficial for illnesses characterized by a significant incubation (latent) phase, such as COVID-19, measles, and influenza [3]. By incorporating an explicitly exposed compartment, the SEIR framework builds upon the classic SIR model, offering a more detailed account of individuals who are infected but not yet contagious. This additional realism improves our ability to simulate disease transmission and design effective public health strategies.

Epidemics with a pronounced incubation stage (e.g., measles, influenza, COVID-19) are naturally

described by an SEIR structure because the explicit exposed class captures infected but not yet infectious individuals and improves realism over SIR when designing control strategies. At the same time, real outbreaks exhibit memory and heredity variable incubation and infectious periods, delayed immune responses, and lingering effects of past contacts, which classical integer-order models cannot represent. Fractional operators address this by letting current dynamics depend on the full history. Among them, the CF family uses a non-singular exponential kernel to model exponentially fading memory and is numerically convenient, but its kernel is not normalized. Therefore, we adopt the NCF derivative, whose kernel integrates to one, aligning the operator with a physical weighted average of past states and improving scaling, interpretability, and often stability of simulations. In the SEIR setting, this normalization matters: it changes the weighting of historical exposures, can delay and flatten infectious peaks, and yields trajectories that more closely reflect gradual, memory-driven epidemic waves. Furthermore, as $\alpha \to 1$, the model recovers the classical SEIR system. To our knowledge, applying the NCF operator within SEIR and analyzing the existence, uniqueness, positivity, conservation, and numerics in one framework fills a gap in the literature and clarifies when normalized memory provides predictive advantages over classical and unnormalized fractional models.

Despite the success of classical integer-order SEIR models, they often fall short in representing the memory and hereditary effects observed in real epidemics, such as variable incubation and infectious periods, delayed immune responses, and the lingering impact of past exposures [4,5]. To address these challenges, fractional-order differential equations have gained traction in epidemiological modeling [5, 6]. The use of fractional derivatives introduces a memory effect, enabling the system's current state to depend on its entire history. This feature frequently results in models that align more closely with empirical data, capturing the complex temporal dynamics of real epidemics [4].

Researchers have introduced numerous concepts of fractional derivatives over the years. The Caputo derivative, with its power-law kernel, is widely adopted for its mathematical properties, but the associated singular kernel can create analytical and numerical difficulties. To address these, the Caputo-Fabrizio (CF) derivative was introduced, featuring a non-singular exponential kernel [7, 8]. This derivative has been applied in numerous fields including epidemiology due to its ability to model processes with exponentially fading memory and its computational advantages [9–11]. Fractional modeling has become a powerful way to capture memory and hereditary effects in dynamical and epidemic systems, supported by advances in optimal control and higher-order solvers for fractional ODEs [12–14]. In epidemiology, normalized non-singular kernels, especially the normalized Caputo–Fabrizio operator, clarify how fractional-order shapes timing and peak size, and pair well with data-driven methods across COVID-19 [15], SIQR [16], and other applications [17, 18]. Building on this literature, we analyze how kernel normalization and finite memory influence SEIR dynamics and the interpretation of interventions.

Nonetheless, the original CF kernel is not normalized, which may cause inconsistencies in the interpretation of memory effects and in the scaling of solutions. To address these issues, the NCF derivative was proposed, where the kernel is constructed to integrate to unity [19]. This normalization not only aligns the operator with the physical concept of averaging but also potentially improves the stability and accuracy of fractional models.

Although the NCF derivative offers theoretical and practical advantages, its application has not yet been systematically studied in the context of SEIR epidemic models. The present study aims to formulate, analyze, and numerically investigate the SEIR epidemic model using the NCF derivative.

We establish a comprehensive theoretical analysis, addressing existence, uniqueness, positivity, and boundedness of solutions, develop an efficient numerical scheme, and present simulations that compare the NCF-SEIR model with classical and standard CF-SEIR models.

This study aims to develop a robust fractional SEIR model based on the NCF derivative, analyze its mathematical characteristics, and illustrate its effectiveness in representing realistic epidemic patterns through detailed numerical experiments.

Section 2 reviews the necessary preliminaries on fractional derivatives. Section 3 presents the model formulation. Section 4 contains the theoretical analysis with step-by-step proofs. Section 5 introduces the numerical method. Section 6 discusses simulation results and comparison with standard models. Section 7 offers final comments and suggestions for future research.

2. Preliminaries

Before proceeding, we present the following definitions, which will be fundamental in the development of our main results.

Definition 2.1. *[7] For $0 < \alpha < 1$, the CF derivative of a function $u(t)$ is*

$$({}^{CF}D_0^{\alpha}u)(t) = \frac{1}{1-\alpha}\int_0^t e^{-\mu_\alpha(t-s)}u'(s)ds,$$

where $\mu_\alpha = \frac{\alpha}{1-\alpha}$.

Definition 2.2. *[20] The NCF derivative is defined by*

$$({}^{NCF}D_0^{\alpha}u)(t) = \frac{1}{(1-\alpha)C_\alpha(t)}\int_0^t e^{-\mu_\alpha(t-s)}u'(s)ds,$$

where

$$C_\alpha(t) = \frac{1}{\alpha}(1-e^{-\mu_\alpha t}).$$

This normalization ensures the kernel integrates to 1 over $[0,t]$.

3. Model formulation

We consider the normalized fractional SEIR model:

$$\begin{aligned}
({}^{NCF}D_0^{\alpha}S)(t) &= -\beta S(t)I(t),\\
({}^{NCF}D_0^{\alpha}E)(t) &= \beta S(t)I(t) - \sigma E(t),\\
({}^{NCF}D_0^{\alpha}I)(t) &= \sigma E(t) - \gamma I(t),\\
({}^{NCF}D_0^{\alpha}R)(t) &= \gamma I(t),\\
S(0) = S_0 \geq 0,\ E(0) = E_0 \geq 0,\ I(0) = I_0 \geq 0,\ R(0) &= R_0 \geq 0,
\end{aligned} \tag{3.1}$$

where, β denotes the transmission coefficient, σ indicates the transition rate from exposed to infectious, and γ represents the rate of recovery. The total population is $N_0 = S_0 + E_0 + I_0 + R_0$.

Within this modeling framework, $S(t)$, $E(t)$, $I(t)$, and $R(t)$ describe, respectively, the fractions of the population that are susceptible, exposed (not yet infectious), currently infectious, and recovered at any given time t. The notation ${}^{NCF}D_0^{\alpha}$ refers to the normalized Caputo-Fabrizio fractional derivative of order α with $0 < \alpha < 1$. This fractional derivative introduces memory effects into the system via a normalized, non-singular kernel, thereby enabling the model to reflect how previous states influence current epidemic dynamics.

The first equation models the rate at which susceptible individuals become exposed to the infection, driven by contact with infectious individuals at a rate determined by β. The second equation describes the progression of exposed individuals to the infectious class at a rate σ, as well as their depletion due to becoming infectious. The third equation accounts for the increase in infectious individuals coming from the exposed class and their removal through recovery at a rate γ. The fourth equation captures the accumulation of recovered individuals. The initial conditions S_0, E_0, I_0, and R_0 set the starting distribution of the population among the four compartments, with all variables assumed nonnegative and summing to the total population N_0.

By extending the classical SEIR model with the NCF derivative, this formulation allows for memory effects that are often present in real-world epidemics, such as latency periods, temporary immunity, and behavioral adaptation over time. As $\alpha \to 1$, the NCF-SEIR model recovers the classical SEIR model with integer-order derivatives. The use of the normalized kernel ensures that the overall memory contribution remains well-scaled and avoids the mathematical singularities of classical fractional operators, thereby improving the model's ability to capture and predict realistic epidemic processes.

4. Theoretical analysis

We establish the existence and uniqueness of solutions to the NCF-SEIR system, providing a foundation for the model's mathematical validity. The demonstration relies on fixed-point theory and essential characteristics of the NCF fractional operator.

4.1. Existence and uniqueness of solutions

Before analyzing the dynamics, we establish that the NCF-SEIR model admits a unique global solution. This guarantees the mathematical consistency and reliability of the system.

Theorem 1. *There exists a unique global solution* (S, E, I, R) *to the NCF-SEIR system on* $[0, T]$.

Proof. We rewrite the NCF-SEIR model using properties of the NCF operator (see [8]):

$$S(t) = S_0 + (1-\alpha)C_\alpha(t)\left[-\beta S(t)I(t)\right] + \alpha\int_0^t C_\alpha(\tau)\left[-\beta S(\tau)I(\tau)\right]d\tau,$$

$$E(t) = E_0 + (1-\alpha)C_\alpha(t)\left[\beta S(t)I(t) - \sigma E(t)\right] + \alpha\int_0^t C_\alpha(\tau)\left[\beta S(\tau)I(\tau) - \sigma E(\tau)\right]d\tau,$$

$$I(t) = I_0 + (1-\alpha)C_\alpha(t)\left[\sigma E(t) - \gamma I(t)\right] + \alpha\int_0^t C_\alpha(\tau)\left[\sigma E(\tau) - \gamma I(\tau)\right]d\tau,$$

$$R(t) = R_0 + (1-\alpha)C_\alpha(t)\left[\gamma I(t)\right] + \alpha\int_0^t C_\alpha(\tau)\left[\gamma I(\tau)\right]d\tau,$$

where $C_\alpha(t)$ is the normalization function of the kernel.

Let $X = [C([0,T])]^4$, the Banach space of continuous vector-valued functions on $[0,T]$ with norm

$$\|U\| = \max\{\|S\|_\infty, \|E\|_\infty, \|I\|_\infty, \|R\|_\infty\}.$$

Define $f_1 = -\beta S I$, $f_2 = \beta S I - \sigma E$, $f_3 = \sigma E - \gamma I$, and $f_4 = \gamma I$.

Define the operator $\mathcal{T}$ on X by:

$$\mathcal{T}\begin{pmatrix} S \\ E \\ I \\ R \end{pmatrix}(t) = \begin{pmatrix} S_0 + (1-\alpha)C_\alpha(t) f_1(S(t),E(t),I(t),R(t)) + \alpha \int_0^t C_\alpha(\tau) f_1(S(\tau),E(\tau),I(\tau),R(\tau))\, d\tau \\ E_0 + (1-\alpha)C_\alpha(t) f_2(S(t),E(t),I(t),R(t)) + \alpha \int_0^t C_\alpha(\tau) f_2(S(\tau),E(\tau),I(\tau),R(\tau))\, d\tau \\ I_0 + (1-\alpha)C_\alpha(t) f_3(S(t),E(t),I(t),R(t)) + \alpha \int_0^t C_\alpha(\tau) f_3(S(\tau),E(\tau),I(\tau),R(\tau))\, d\tau \\ R_0 + (1-\alpha)C_\alpha(t) f_4(S(t),E(t),I(t),R(t)) + \alpha \int_0^t C_\alpha(\tau) f_4(S(\tau),E(\tau),I(\tau),R(\tau))\, d\tau \end{pmatrix}$$

We will show $\mathcal{T}$ is a contraction on a suitable subset of X by proving each f_j is Lipschitz continuous on bounded sets. Let $D_M = \{(S,E,I,R) \in X : \|S\|, \|E\|, \|I\|, \|R\| \le M\}$ for some $M > 0$ for all $(S_1,E_1,I_1,R_1), (S_2,E_2,I_2,R_2)$ in D_M:

$$\begin{aligned} |f_1(S_1,E_1,I_1,R_1) - f_1(S_2,E_2,I_2,R_2)| &= |-\beta S_1 I_1 + \beta S_2 I_2| \\ &= \beta |S_2 I_2 - S_1 I_1| \\ &= \beta |S_2(I_2 - I_1) + (S_2 - S_1) I_1| \\ &\le \beta(|S_2||I_2 - I_1| + |I_1||S_2 - S_1|) \\ &\le 2\beta M \|(S_1,E_1,I_1,R_1) - (S_2,E_2,I_2,R_2)\| \end{aligned}$$

$$\begin{aligned} |f_2(S_1,E_1,I_1,R_1) - f_2(S_2,E_2,I_2,R_2)| &= |\beta S_1 I_1 - \sigma E_1 - [\beta S_2 I_2 - \sigma E_2]| \\ &= |\beta(S_1 I_1 - S_2 I_2) - \sigma(E_1 - E_2)| \\ &\le \beta(|S_1||I_1 - I_2| + |I_2||S_1 - S_2|) + \sigma|E_1 - E_2| \\ &\le (2\beta M + \sigma)\|(S_1,E_1,I_1,R_1) - (S_2,E_2,I_2,R_2)\| \end{aligned}$$

$$\begin{aligned} |f_3(S_1,E_1,I_1,R_1) - f_3(S_2,E_2,I_2,R_2)| &= |\sigma E_1 - \gamma I_1 - [\sigma E_2 - \gamma I_2]| \\ &= |\sigma(E_1 - E_2) - \gamma(I_1 - I_2)| \\ &\le \sigma|E_1 - E_2| + \gamma|I_1 - I_2| \\ &\le (\sigma + \gamma)\|(S_1,E_1,I_1,R_1) - (S_2,E_2,I_2,R_2)\| \end{aligned}$$

$$\begin{aligned} |f_4(S_1,E_1,I_1,R_1) - f_4(S_2,E_2,I_2,R_2)| &= |\gamma I_1 - \gamma I_2| = \gamma|I_1 - I_2| \\ &\le \gamma\|(S_1,E_1,I_1,R_1) - (S_2,E_2,I_2,R_2)\|. \end{aligned}$$

Let L_M be the largest of the coefficients above. For any $U_1, U_2 \in D_M$,

$$\|\mathcal{T}(U_1) - \mathcal{T}(U_2)\| \le K L_M \|U_1 - U_2\|,$$

where K depends on T, α, and the kernel normalization. By choosing T sufficiently small so that $KL_M < 1$, $\mathcal{T}$ is a contraction on D_M.

By Banach's fixed-point theorem, there is a unique fixed point (solution) in D_M on $[0, T_0]$ for some $T_0 > 0$.

Since the solutions remain nonnegative and bounded by the total population, the local solution can be extended step-by-step to the whole interval $[0,T]$.

□

4.2. Positivity of solutions

Before proceeding, it is essential to verify that the solutions of the NCF-SEIR model remain nonnegative for all time, as required by the biological interpretation of the compartments.

Theorem 2. *If $S_0, E_0, I_0, R_0 \geq 0$, then $S(t), E(t), I(t), R(t) \geq 0$ for all $t \geq 0$.*

Proof. Assume, for the sake of contradiction, that there is an initial time $t^* > 0$ at which one of the state variables $S(t^*)$, $E(t^*)$, $I(t^*)$, or $R(t^*)$ reaches zero, having remained nonnegative for all earlier times $t < t^*$.

Examine each equation at t^*:

- The equation for $S(t)$ has right-hand side $-\beta S(t)I(t) \leq 0$, so $S(t)$ cannot decrease below zero.
- The equation for $E(t)$ is $\beta S(t)I(t) - \sigma E(t)$. When $E(t^*) = 0$, this reduces to $\beta S(t^*)I(t^*) \geq 0$.
- The equation for $I(t)$ is $\sigma E(t) - \gamma I(t)$. When $I(t^*) = 0$, this reduces to $\sigma E(t^*) \geq 0$.
- The equation for $R(t)$ is $\gamma I(t) \geq 0$.

In each case, the right-hand sides are nonnegative (or zero) at the boundary $S = 0$, $E = 0$, $I = 0$, or $R = 0$. Thus, the NCF derivative cannot make the solution decrease below zero at this first hitting time, and so a contradiction is reached.

Therefore, solutions must remain nonnegative for all $t \geq 0$. □

4.3. Boundedness

It is essential to ensure that the total population remains bounded and conserved over time. We establish that the sum of all compartments in the NCF–SEIR model does not exceed the initial population.

Lemma 4.1. *Let $0 < \alpha < 1$ and suppose u is absolutely continuous on $[0, T]$. Define*

$$({}^{\mathrm{NCF}}D_0^{\alpha}u)(t) = \frac{1}{(1-\alpha)\,C_\alpha(t)} \int_0^t e^{-\mu_\alpha(t-s)}\,u'(s)\,ds, \qquad C_\alpha(t) = \frac{1-e^{-\mu_\alpha t}}{\alpha},\ \ \mu_\alpha = \frac{\alpha}{1-\alpha}.$$

If $({}^{\mathrm{NCF}}D_0^{\alpha}u)(t) = 0$ for all $t \in (0, T]$, then u is constant on $[0, T]$. In particular, if $u(0) = c$, then $u(t) \equiv c$ on $[0, T]$.

Proof. Let $v(t) := \int_0^t e^{-\mu_\alpha(t-s)}\,u'(s)\,ds$. For $t > 0$, we have $(1-\alpha)C_\alpha(t) > 0$, hence $({}^{\mathrm{NCF}}D_0^{\alpha}u)(t) = 0$ implies $v(t) \equiv 0$ on $(0, T]$. Since $u' \in L^1(0, T)$, v is absolutely continuous and differentiation under the integral yields, for a.e. $t \in (0, T]$,

$$v'(t) = u'(t) - \mu_\alpha \int_0^t e^{-\mu_\alpha(t-s)}\,u'(s)\,ds = u'(t) - \mu_\alpha v(t) = u'(t).$$

Thus, $0 = v'(t) = u'(t)$ a.e. on $(0, T]$, so u is constant on $[0, T]$. □

Theorem 3. *Let $N(t) = S(t) + E(t) + I(t) + R(t)$. Then, $N(t) \equiv N_0$ for all $t \geq 0$. Consequently, if the dynamics preserve nonnegativity of the compartments, $0 \leq S(t), E(t), I(t), R(t) \leq N_0$ for all $t \geq 0$.*

Proof. Summing the four equations of the NCF–SEIR system gives

$$({}^{\mathrm{NCF}}D_0^{\alpha}S)(t) + ({}^{\mathrm{NCF}}D_0^{\alpha}E)(t) + ({}^{\mathrm{NCF}}D_0^{\alpha}I)(t) + ({}^{\mathrm{NCF}}D_0^{\alpha}R)(t) = 0.$$

By the linearity of the NCF derivative,

$$({}^{\mathrm{NCF}}D_0^{\alpha}N)(t) = 0.$$

By the lemma 4.1 and the initial condition $N(0) = N_0$, we conclude $N(t) \equiv N_0$ for all $t \geq 0$. If, in addition, the vector field leaves the nonnegative invariant, then $S, E, I, R \geq 0$, and hence each is bounded above by N_0. □

Remark 4.2. *If N_1 and N_2 satisfy $({}^{\mathrm{NCF}}D_0^{\alpha}N_i)(t) = 0$ with $N_1(0) = N_2(0)$, then $({}^{\mathrm{NCF}}D_0^{\alpha}(N_1 - N_2))(t) = 0$ and $(N_1 - N_2)(0) = 0$, so by the lemma 4.1 $N_1 \equiv N_2$.*

Population conservation holds as stated when the sum of the right-hand sides of the compartmental equations is identically zero. If demographic terms are included, e.g., $({}^{\mathrm{NCF}}D_0^{\alpha}N)(t) = \Lambda(t) - \mu(t)N(t)$, then N is generally not constant, though analogous bounds can be derived by comparison.

4.4. Equilibria and disease-free invariance

Setting all derivatives to zero, the system yields $I^* = 0$ and $E^* = 0$, with $S^* + R^* = N_0$; thus, the only equilibrium is the disease-free state. If $I_0 = 0$ and $E_0 = 0$, all solutions remain disease-free for all time.

4.5. Stability of the disease-free equilibrium

Next, we examine the stability of the disease-free equilibrium (DFE) to determine the conditions under which the infection dies out in the NCF-SEIR model.

Theorem 4. *Consider the NCF-SEIR model. The equilibrium point $(S^*, E^*, I^*, R^*) = (N_0, 0, 0, 0)$, corresponding to the absence of infection, is locally asymptotically stable whenever the basic reproduction number $\mathcal{R}_0 = \frac{\beta N_0}{\gamma}$ satisfies $\mathcal{R}_0 < 1$. If instead $\mathcal{R}_0 > 1$, this equilibrium becomes unstable.*

Proof. Recall the NCF-SEIR system:

$$\begin{aligned}
({}^{NCF}D_0^{\alpha}S)(t) &= -\beta S(t)I(t),\\
({}^{NCF}D_0^{\alpha}E)(t) &= \beta S(t)I(t) - \sigma E(t),\\
({}^{NCF}D_0^{\alpha}I)(t) &= \sigma E(t) - \gamma I(t),\\
({}^{NCF}D_0^{\alpha}R)(t) &= \gamma I(t).
\end{aligned}$$

The DFE is $(S^*, E^*, I^*, R^*) = (N_0, 0, 0, 0)$.

Consider small perturbations near the DFE:

$$S(t) = N_0 + s(t), \quad E(\upsilon) = N_0 + e(t), \quad I(t) = N_0 + i(t), \quad R(t) = N_0 + r(t)$$

where $|s(t)|, |e(t)|, |i(t)|$ and $|r(t)|$ are small.

Linearizing around the DFE and neglecting higher-order terms, we have:

$$({}^{NCF}D_0^{\alpha}s)(t) = -\beta N_0 i(t),$$

$$
\begin{aligned}
({}^{NCF}D_0^{\alpha} e)(t) &= \beta N_0 i(t) - \sigma e(t),\\
({}^{NCF}D_0^{\alpha} i)(t) &= \sigma e(t) - \gamma i(t),\\
({}^{NCF}D_0^{\alpha} r)(t) &= \gamma i(t).
\end{aligned}
$$

We focus on the subsystem involving $e(t)$ and $i(t)$. Let us write it as a vector system:

$$
\begin{pmatrix} ({}^{NCF}D_0^{\alpha} e)(t) \\ ({}^{NCF}D_0^{\alpha} i)(t) \end{pmatrix} = \begin{pmatrix} -\sigma & \beta N_0 \\ \sigma & -\gamma \end{pmatrix} \begin{pmatrix} e(t) \\ i(t) \end{pmatrix}
$$

The stability is determined by the eigenvalues λ of the matrix:

$$
A = \begin{pmatrix} -\sigma & \beta N_0 \\ \sigma & -\gamma \end{pmatrix}
$$

The characteristic equation is:

$$
\det(A - \lambda I) = 0 \implies \begin{vmatrix} -\sigma - \lambda & \beta N_0 \\ \sigma & -\gamma - \lambda \end{vmatrix} = 0
$$

By expanding, we have

$$
(-\sigma - \lambda)(-\gamma - \lambda) - \beta N_0 \sigma = 0
$$

$$
(\lambda + \sigma)(\lambda + \gamma) - \beta N_0 \sigma = 0
$$

$$
\lambda^2 + (\sigma + \gamma)\lambda + \sigma\gamma - \beta N_0 \sigma = 0
$$

$$
\lambda^2 + (\sigma + \gamma)\lambda + \sigma\gamma(1 - \mathcal{R}_0) = 0, \quad \text{where} \quad \mathcal{R}_0 = \frac{\beta N_0}{\gamma}
$$

For stability, all roots of this quadratic must have negative genuine parts, which holds if and only if $\mathcal{R}_0 < 1$ by the Routh-Hurwitz criterion.

Thus:

- If $\mathcal{R}_0 < 1$, all solutions decay to zero, and the DFE is locally asymptotically stable.
- If $\mathcal{R}_0 > 1$, at least one eigenvalue has a positive real part, and the DFE is unstable.

□

5. Numerical method

Let $T > 0$ be the final simulation time and $N \in \mathbb{N}$ the total number of time steps. Define the uniform grid with step size $h = T/N$ and $t_n = nh$, $n = 0, 1, \ldots, N$. Throughout, set

$$
C_{\alpha}(t) = \frac{1 - e^{-\mu_{\alpha} t}}{\alpha}, \qquad \mu_{\alpha} = \frac{\alpha}{1 - \alpha}, \qquad \alpha \in (0, 1).
$$

5.1. Discretization of the NCF derivative

For any scalar sequence $\{u_n\}$ define the exponentially weighted running difference

$$W_n^{(u)} \;=\; e^{-\mu_\alpha h}\, W_{n-1}^{(u)} \;+\; (u_n - u_{n-1}), \qquad W_0^{(u)} := 0. \tag{5.1}$$

We approximate the NCF derivative at t_n by

$$({}^{\mathrm{NCF}}D_0^\alpha u)(t_n) \;\approx\; \frac{W_n^{(u)}}{(1-\alpha)\, C_\alpha(t_n)}. \tag{5.2}$$

The recurrence (5.1)–(5.2) yields $O(N)$ *time* and $O(1)$ *memory*. It is algebraically equivalent to the rectangle-rule history sum (shown for reference only):

$$({}^{\mathrm{NCF}}D_0^\alpha u)(t_n) \;\approx\; \frac{1}{(1-\alpha)\, C_\alpha(t_n)} \sum_{k=0}^{n-1} e^{-\mu_\alpha(t_n - t_k)}\, [u_{k+1} - u_k], \tag{5.3}$$

but (5.1) is better conditioned when $\alpha \to 1$.

As $\alpha \to 1$, the NCF operator converges to the classical first derivative. Numerically, using the $O(N)$ recurrence (5.1)–(5.2) avoids cancellation when $(1-\alpha)$ is small; in this limit, the update approaches explicit Euler.

5.2. Explicit scheme for the NCF–SEIR system

Let $U = (S, E, I, R)^\top$ and

$$F(U) = \left[-\beta S I,\ \beta S I - \sigma E,\ \sigma E - \gamma I,\ \gamma I\right]^\top.$$

We discretize the right-hand side with explicit Euler to form the per-step increments

$$\begin{aligned} S_n - S_{n-1} &= -h\beta S_{n-1} I_{n-1}, \\ E_n - E_{n-1} &= h\,[\beta S_{n-1} I_{n-1} - \sigma E_{n-1}], \\ I_n - I_{n-1} &= h\,[\sigma E_{n-1} - \gamma I_{n-1}], \\ R_n - R_{n-1} &= h\,\gamma I_{n-1}. \end{aligned} \tag{5.4}$$

These increments are inserted into (5.1) componentwise to update $W_n^{(S)}, W_n^{(E)}, W_n^{(I)}$ and $W_n^{(R)}$, and the NCF derivatives are then read off via (5.2):

$$({}^{\mathrm{NCF}}D_0^\alpha u)(t_n) \;\approx\; \frac{W_n^{(u)}}{(1-\alpha)\, C_\alpha(t_n)} \quad \text{with } u \in \{S, E, I, R\} \text{ and } W_n^{(u)} \text{ from (5.1) using (5.4).} \tag{5.5}$$

To mitigate step-size restrictions at small α, we use a semi-implicit update that preserves mass and positivity. With step h and states S^n, E^n, I^n and R^n:

$$S^n = \frac{S^{n-1}}{1 + h\beta\, I^{n-1}}, \quad E^n = \frac{E^{n-1} + h\beta\, S^n I^{n-1}}{1 + h\sigma}, \quad I^n = \frac{I^{n-1} + h\sigma\, E^n}{1 + h\gamma}, \quad R^n = R^{n-1} + h\gamma\, I^n.$$

The NCF derivative is evaluated with the same exponentially weighted history accumulator as in the main text. This scheme is mass-conserving ($S^n + E^n + I^n + R^n = N_0$) and positivity-preserving for any

$h > 0$. On our test problems, it remains stable and non-oscillatory for $\alpha < 0.5$ with step sizes several times larger than those admissible for the explicit update. It produces trajectories consistent with the explicit scheme under refinement.

Algorithm:

i) Evaluate $F(U_{n-1})$ and set $U_n = U_{n-1} + h\,F(U_{n-1})$ (explicit Euler; produces (5.4)).

ii) Update $W_n^{(u)}$ by (5.1) with the just-computed $u_n - u_{n-1}$.

iii) (Optional, for diagnostics) Compute $({}^{\mathrm{NCF}}D_0^{\alpha}u)(t_n)$ via (5.2).

The continuous model preserves $S, E, I, R \geq 0$ and $S + E + I + R = N_0$. Explicit Euler requires a step-size restriction to retain $S_n, E_n, I_n, R_n \geq 0$. A sufficient bound is

$$h \;\leq\; \frac{\theta}{\beta N_0 + \sigma + \gamma}, \qquad \theta \in (0, 1], \tag{5.6}$$

which ensures that each increment in (5.4) is a nonnegative combination of current states and keeps all compartments nonnegative.

5.3. Convergence analysis

Assume the NCF–SEIR solution exists on $[0, T]$ and remains in the positively invariant set

$$\mathcal{D} = \{U \in \mathbb{R}^4_{\geq 0} : \; \|U\|_1 = N_0\},$$

and F is globally Lipschitz on $\mathcal{D}$ with constant L. Consider the scheme (5.4)+(5.1)+(5.5) under the step-size condition (5.6).

Theorem 5. *There exist $h_0 > 0$ and $C_T > 0$, depending on $T, \alpha, \beta, \sigma, \gamma$ and N_0 but not on h, such that for all $0 < h \leq h_0$,*

$$\max_{0 \leq n \leq N} \|U(t_n) - U_n\| \;\leq\; C_T\, h.$$

Hence, the method is first-order accurate in time.

Proof. Write the exact NCF operator as

$$({}^{\mathrm{NCF}}D_0^{\alpha}U)(t_n) = \frac{1}{(1-\alpha)\,C_\alpha(t_n)} \int_0^{t_n} e^{-\mu_\alpha(t_n - s)}\, U'(s)\, ds.$$

Applying the left-point rectangle rule on each $[t_k, t_{k+1}]$ gives

$$\frac{1}{(1-\alpha)\,C_\alpha(t_n)} \int_0^{t_n} e^{-\mu_\alpha(t_n - s)}\, U'(s)\, ds = \frac{1}{(1-\alpha)\,C_\alpha(t_n)} \sum_{k=0}^{n-1} e^{-\mu_\alpha(t_n - t_k)}(U(t_{k+1}) - U(t_k)) + \tau_n,$$

with $\|\tau_n\| \leq C_T h$ (smooth kernel and U'' bounded). Using the model ${}^{\mathrm{NCF}}D_0^{\alpha}U = F(U)$ and the scheme identity obtained by replacing the exact increments with the numerical ones $U_{k+1} - U_k = hF(U_k)$, we arrive at

$$F(U(t_n)) - F(U_n) = \sum_{k=0}^{n-1} \omega_{n,k}\,(e_{k+1} - e_k) + \tau_n,$$

where $e_n = U(t_n) - U_n$ and $\omega_{n,k} = \frac{e^{-\mu_\alpha(t_n - t_k)}}{(1-\alpha)\,C_\alpha(t_n)}$. Lipschitz continuity and a summation-by-parts argument yield

$$\|e_n\| \;\le\; C \sum_{k=0}^{n-1} e^{-\mu_\alpha(t_n - t_{k+1})} \|e_k\| \;+\; C\,\|\tau_n\|.$$

A discrete Grönwall inequality with exponentially decaying weights (and the stability implied by (5.6)) gives $\|e_n\| \le C_T(\|e_0\| + \max_{1\le j\le n} \|\tau_j\|) \le C_T h$, proving the claim. □

Replacing the rectangle rule in (5.3) by a trapezoidal correction inside the history integral yields a global $O(h^2)$ scheme under the same assumptions and a similar explicit CFL restriction.

5.4. Consistency and accuracy

- The baseline scheme (5.4)+(5.1)+(5.5) is first-order accurate in h.
- A trapezoidal history integral upgrades the order to two without making the whole method implicit.
- As $\alpha \to 1$, the $O(N)$ recurrence avoids cancellation and the update approaches classical explicit Euler.

5.5. Comparison with standard Caputo and CF

For context, one may compare against the standard Caputo discretization and the unnormalized CF model. The NCF normalization keeps the total memory weight equal to one, which can shift timing and height of epidemic peaks relative to the unnormalized and power-law cases while preserving interpretability.

6. Numerical simulations and discussion

We investigate how fractional memory and kernel normalization shape epidemic dynamics in the SEIR model. Unless otherwise stated, the parameters are

$$\beta = 0.4, \quad \gamma = 0.15, \quad \sigma = 0.2, \quad (S_0, E_0, I_0, R_0) = (0.95,\ 0.02,\ 0.02,\ 0.01),$$

with final time $T = 25$ days and step size $h = 0.05$. Fractional orders $\alpha \in \{0.95, 0.85, 0.75, 0.40, 0.30\}$ span the range from nearly classical to strong-memory regimes. All NCF runs use the $O(N)$ history recurrence; for $\alpha < 0.5$, we use the semi-implicit variant, which gives stable, non-oscillatory trajectories without minimal time steps and is consistent with the explicit update under refinement.

Figure 1 shows the four classical SEIR compartments, providing the reference time scale for comparisons. Figure 2 displays NCF trajectories as α varies: decreasing α delays and flattens the epidemic wave peaks in $I(t)$ and $E(t)$ occur later and at lower amplitudes, $S(t)$ depletes more gradually, and $R(t)$ accumulates more slowly. As $\alpha \to 1$, the NCF curves approach the classical limit.

The peak surfaces in Figure 3 summarizes these trends over (α, β). Holding β fixed, smaller α suppresses I_{peak} and E_{peak}; holding α fixed, larger β raises them. The R_{peak} surface tracks I_{peak}, while S_{peak} decreases as either β or α increases, reflecting faster susceptible depletion.

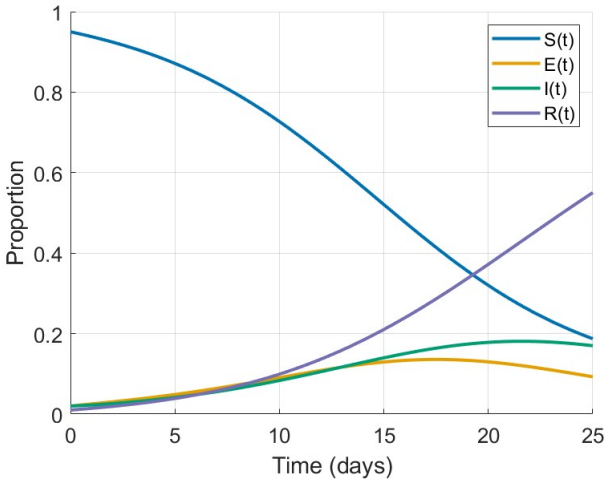

Figure 1. The classical SEIR model 3.1.

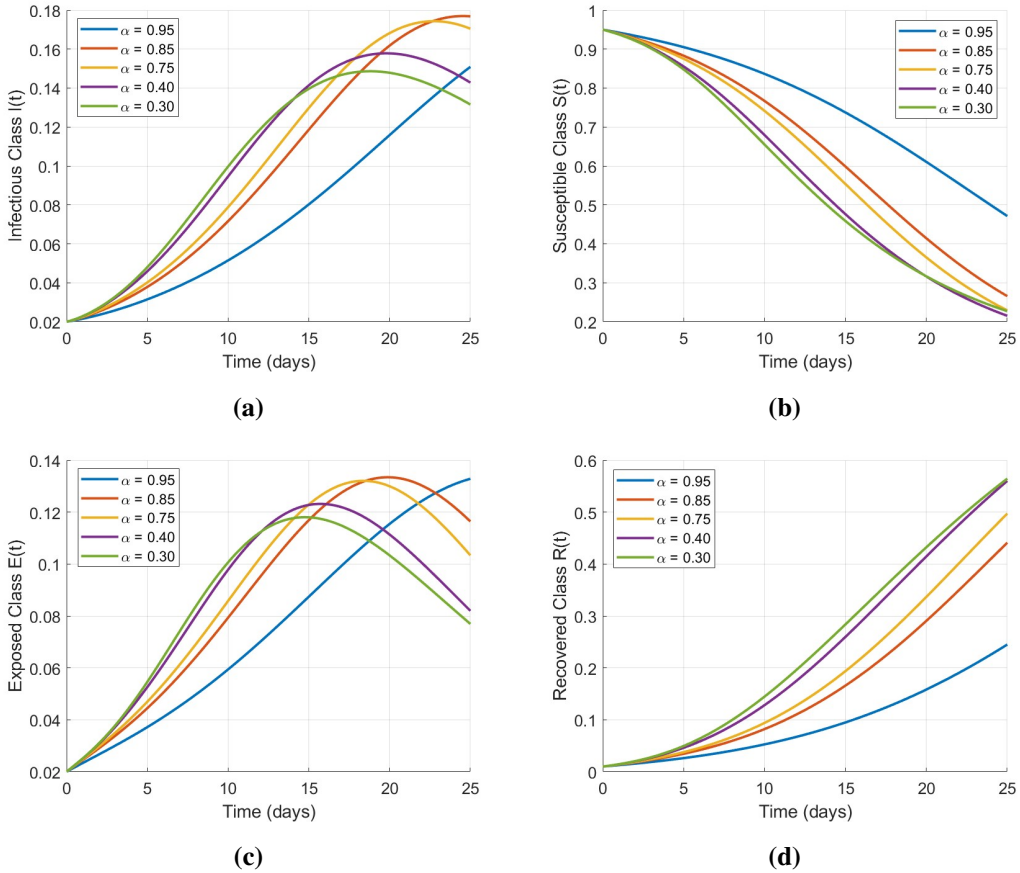

Figure 2. NCF–SEIR trajectories for varying fractional order α: (a) Infectious $I(t)$, (b) Susceptible $S(t)$, (c) Exposed $E(t)$, (d) Recovered $R(t)$.

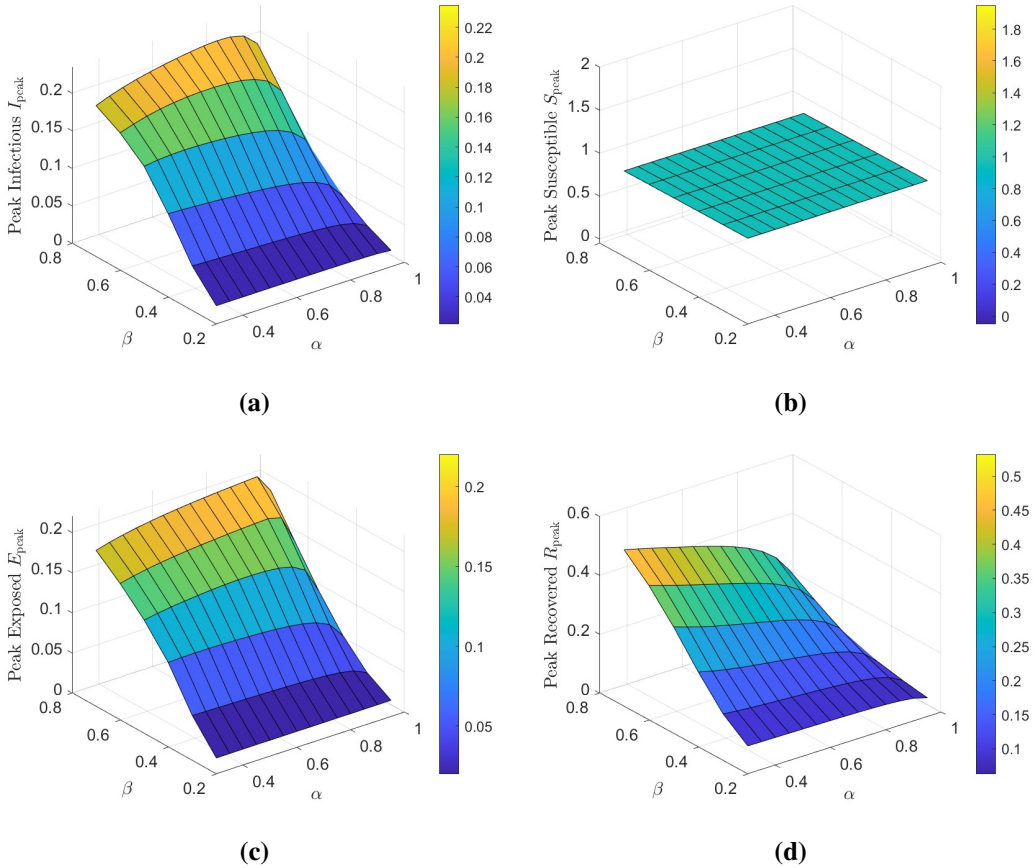

Figure 3. Peak values versus fractional order α and infection rate β: (a) Infectious I_{peak}, (b) Susceptible S_{peak}, (c) Exposed E_{peak}, and (d) Recovered R_{peak}. Surfaces show how peak magnitudes vary jointly with α and β.

Figure 4 contrasts the four formulations Classical, Caputo, CF (unnormalized), and NCF across $\alpha = \{0.95, 0.85, 0.75, 0.40, 0.30\}$. Classical shows the fastest rise permitted by h. Caputo delays and damps the wave as α decreases. The unnormalized CF model exhibits aggressive early growth and rapid saturation under the same parameters, a scaling artifact of the non-normalized kernel. In contrast, NCF is well-scaled and produces delayed, lower peaks than Classical and CF while qualitatively aligning with Caputo at the same α. These patterns are consistent with the quantitative summary in Table 1: e.g., at $\alpha = 0.95$, the NCF infectious peak is markedly below Classical while occurring on a comparable time scale, whereas the unnormalized CF reports unit-scale spikes with very short durations.

Sensitivity tests in Figure 5 show that perturbing a single initial compartment mainly influences the initial rise: increasing E_0 or I_0 elevates and slightly advances the early $E(t)$ or $I(t)$; increasing S_0 accelerates depletion and amplifies the ensuing wave; increasing R_0 dampens transmission. In comparison, peak timing and height are governed chiefly by α and by β, σ, and γ.

Overall, the NCF derivative offers a robust and interpretable representation of short-range memory in epidemic transmission. Normalization preserves a probabilistic weighting of recent history, avoids the scaling issues of unnormalized CF, and yields trajectories that smoothly recover the classical limit as $\alpha \to 1$. Combined with the semi-implicit stepping for small α, the NCF–SEIR framework provides

a practical vehicle for studying memory effects and for scenario analysis in public-health forecasting.

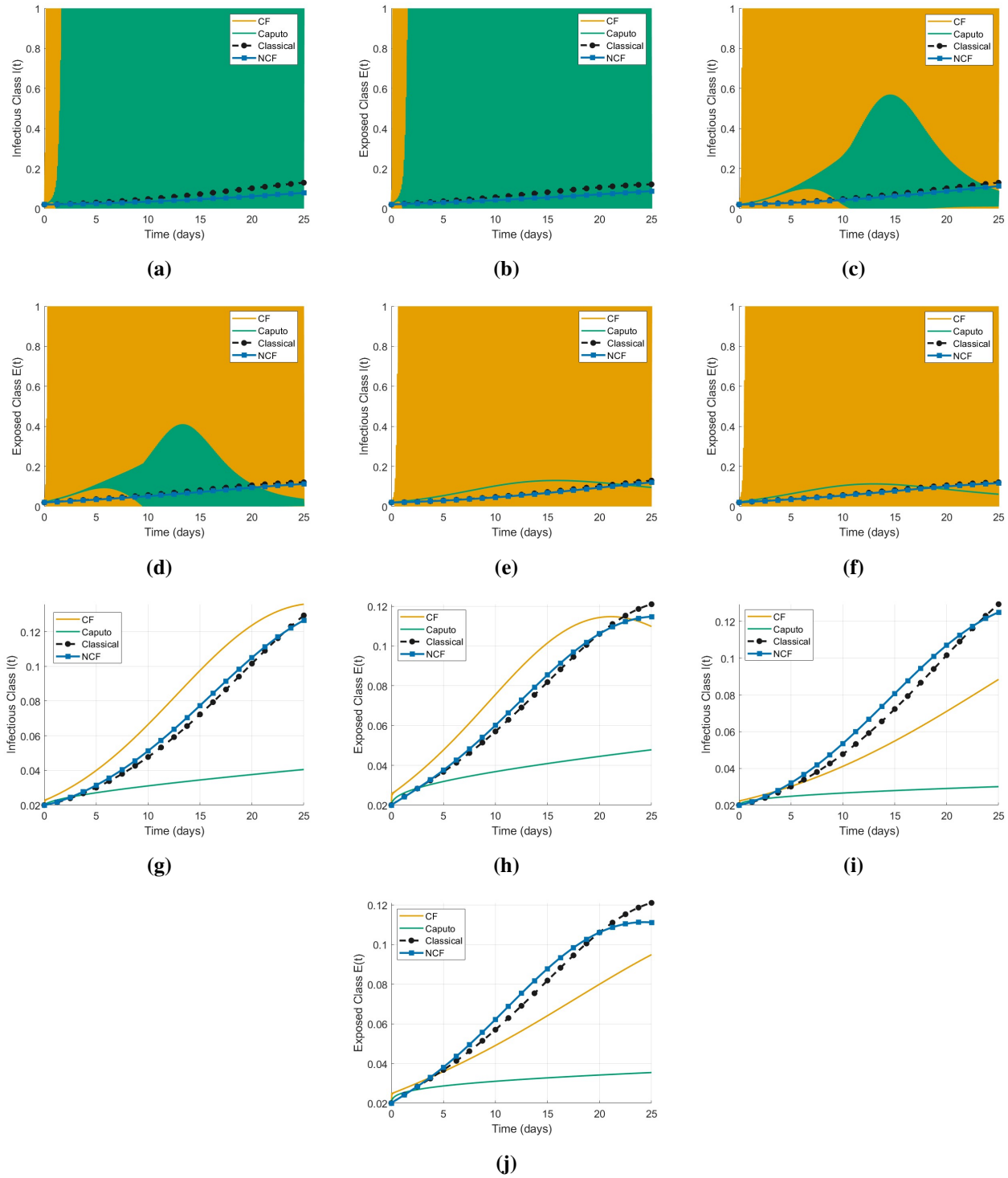

Figure 4. SEIR dynamics across fractional orders. Columns show $\alpha \in \{0.95, 0.85, 0.75, 0.40, 0.30\}$; rows show Infectious $I(t)$ and Exposed $E(t)$. Curves: Classical, Caputo, CF, and NCF. Decreasing α delays and reduces peaks; NCF remains well scaled and aligns with Caputo's damping at the same α.

Table 1. Summary metrics for multi-α comparison figures.

α	Model	I_{peak}	t_{peak}	Final Size	Epidemic Duration
0.95	Classical	0.129360	25.00	0.503570	–
0.95	Caputo	1.000000	1.70	0.000000	1.25
0.95	CF	1.000000	0.20	0.000000	0.15
0.95	NCF	0.078697	25.00	0.281100	–
0.85	Classical	0.129360	25.00	0.503570	–
0.85	Caputo	0.569680	14.60	0.948480	10.75
0.85	CF	1.000000	0.40	0.000000	0.25
0.85	NCF	0.112100	25.00	0.422690	–
0.75	Classical	0.129360	25.00	0.503570	–
0.75	Caputo	0.129900	15.80	0.733280	–
0.75	CF	1.000000	0.70	0.000000	0.35
0.75	NCF	0.120370	25.00	0.464280	–
0.40	Classical	0.129360	25.00	0.503570	–
0.40	Caputo	0.040534	25.00	0.134140	–
0.40	CF	0.135820	25.00	0.622040	–
0.40	NCF	0.126560	25.00	0.523210	–
0.30	Classical	0.129360	25.00	0.503570	–
0.30	Caputo	0.030054	25.00	0.093276	–
0.30	CF	0.088428	25.00	0.325990	–
0.30	NCF	0.124980	25.00	0.536850	–

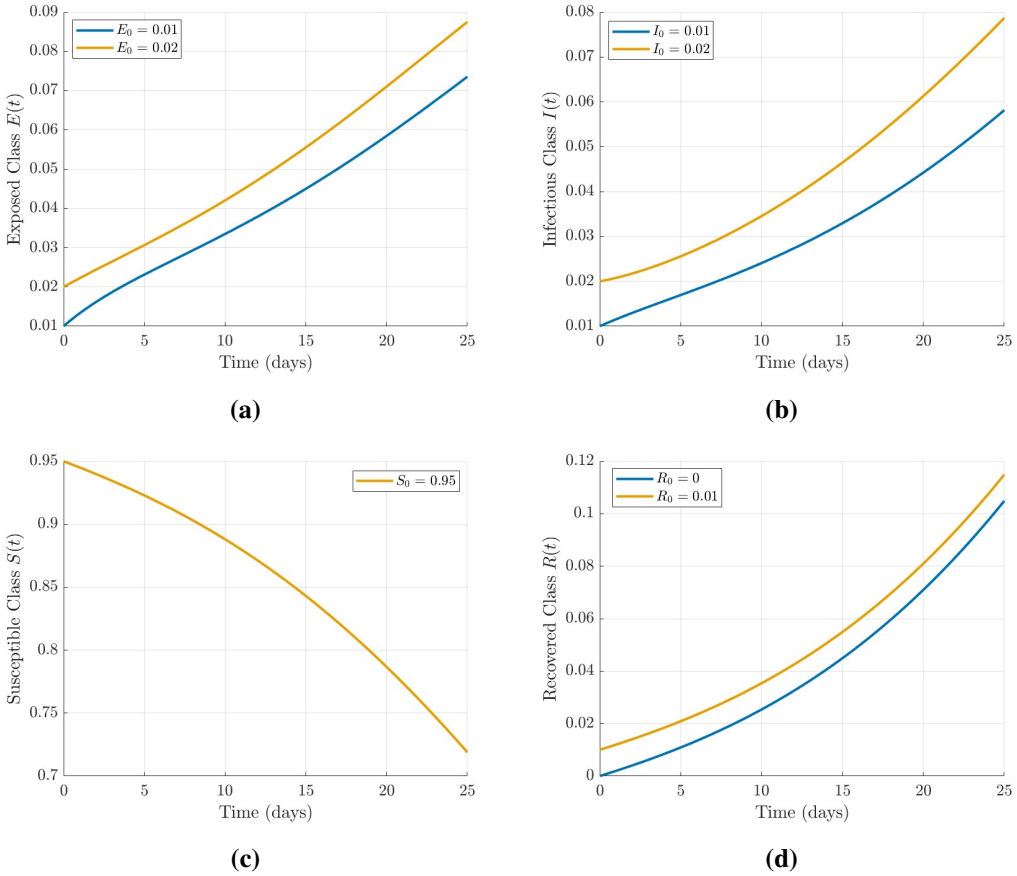

Figure 5. Sensitivity of the NCF–SEIR model to initial conditions. (a) Effect of E_0 on $E(t)$; (b) effect of I_0 on $I(t)$; (c) effect of S_0 on $S(t)$; (d) effect of R_0 on $R(t)$.

7. Conclusions

This work presents the first comprehensive formulation and analysis of the fractional-order SEIR epidemic model utilizing the NCF derivative. We have established key theoretical properties, including existence, uniqueness, positivity, and conservation of the total population, thereby ensuring the mathematical validity of the model. A discrete numerical scheme for the NCF-SEIR model was developed and implemented, enabling a robust investigation of memory effects and kernel normalization on epidemic dynamics. Numerical simulations demonstrate that introducing the normalized memory kernel substantially modifies the qualitative behavior of the epidemic compared to both classical and unnormalized fractional models. Specifically, decreasing the fractional order α results in delayed and flattened epidemic peaks in the exposed and infectious compartments, capturing the gradual spread and persistent memory effects observed in real-world outbreaks. The NCF kernel ensures a physically consistent distribution of memory, leading to more realistic and interpretable epidemic trajectories, particularly in scenarios with significant latency or behavioral adaptation. Sensitivity analyses further confirm that while initial conditions can influence the early phase of an epidemic, the overall shape and progression are primarily governed by the memory parameter and main epidemiological rates. The NCF-SEIR model thus offers a flexible and practical framework for

exploring the impact of memory effects in epidemiological modeling and public health forecasting. Future research directions include parameter estimation from empirical epidemic data to validate the predictive performance of the NCF-SEIR model, as well as extensions to models incorporating vital dynamics, vaccination, control interventions, or more complex multi-stage compartmental structures.

Author contributions

R.S.: Conceptualization, Methodology, Software, Formal analysis, Investigation, Resources, Writing–original draft, Writing–review & editing; S. M. A.: Investigation, Project administration, Funding acquisition; A. A.: Methodology, Software, Resources, Supervision. All authors have read and approved the final version of the manuscript for publication.

Use of Generative-AI tools declaration

The authors declare they have not used Artificial Intelligence (AI) tools in the creation of this article.

Acknowledgments

The authors would like to acknowledge the Deanship of Graduate Studies and Scientific Research, Taif University for funding this work.

Conflict of interest

All authors declare no conflicts of interest in this paper.

References

1. H. W. Hethcote, The mathematics of infectious diseases, *SIAM Rev.*, **42** (2000), 599–653. https://doi.org/10.1137/S0036144500371907
2. F. Brauer, Mathematical epidemiology: past, present, and future, *Infectious Disease Modelling*, **2** (2017), 113–127. https://doi.org/10.1016/j.idm.2017.02.001
3. W. O. Kermack, A. G. McKendrick, A contribution to the mathematical theory of epidemics, *Proc. R. Soc. Lond. A*, **115** (1927), 700–721. https://doi.org/10.1098/rspa.1927.0118
4. K. Diethelm, An investigation of some nonclassical methods for the numerical approximation of Caputo-type fractional derivatives, *Numer. Algor.*, **47** (2008), 361–390. https://doi.org/10.1007/s11075-008-9193-8
5. R. L. Magin, Fractional calculus models of complex dynamics in biological tissues, *Comput. Math. Appl.*, **59** (2010), 1586–1593. https://doi.org/10.1016/j.camwa.2009.08.039
6. H. Sun, A. Chang, Y. Zhang, W. Chen, A review on variable-order fractional differential equations: mathematical foundations, physical models, numerical methods and applications, *Fract. Calc. Appl. Anal.*, **22** (2019), 27–59. https://doi.org/10.1515/fca-2019-0003
7. M. Caputo, M. Fabrizio, A new definition of fractional derivative without singular kernel, *Progress in Fractional Differentiation & Applications*, **1** (2015), 73–85.

8. A. Atangana, D. Baleanu, New fractional derivatives with nonlocal and non-singular kernel: theory and application to heat transfer model, *Therm. Sci.*, **20** (2016), 763–769. https://doi.org/10.2298/TSCI160111018A
9. L. Verma, R. Meher, O. Nikan, A. A. Al-Saedi, Numerical study on fractional order nonlinear SIR-SI model for dengue fever epidemics, *Sci. Rep.*, **15** (2025), 30677. https://doi.org/10.1038/s41598-025-16599-w
10. R. Shafqat, A. Alsaadi, A. Alubaidi, A fractional-order alcoholism model incorporating hypothetical social influence: a theoretical and numerical study, *J. Math.*, **2025** (2025), 6773909. https://doi.org/10.1155/jom/6773909
11. R. Shafqat, A. Alsaadi, Artificial neural networks for stability analysis and simulation of delayed rabies spread models, *AIMS Math.*, **9** (2024), 33495–33531. https://doi.org/10.3934/math.20241599
12. C. Liu, Z. Gong, C. Yu, S. Wang, K. L. Teo, Optimal control computation for nonlinear fractional time-delay systems with state inequality constraints, *J. Optim. Theory Appl.*, **191** (2021), 83–117. https://doi.org/10.1007/s10957-021-01926-8
13. X. Yi, C. Liu, H. T. Cheong, K. L. Teo, S. Wang, A third-order numerical method for solving fractional ordinary differential equations, *AIMS Math.*, **9** (2024), 21125–21143. https://doi.org/10.3934/math.20241026
14. C. Liu, X. Yi, Z. Gong, M. Han, The control parametrization technique for numerically solving fractal-fractional optimal control problems involving Caputo–Fabrizio derivatives, *J. Comput. Appl. Math.*, **472** (2026), 116814. https://doi.org/10.1016/j.cam.2025.116814
15. Y. Hwang, S. Kwak, Jyoti, J. Kim, Optimal time-dependent SUC model for COVID-19 pandemic in India, *BMC Infect. Dis.*, **24** (2024), 1031. https://doi.org/10.1186/s12879024-09961-2
16. R. Shafqat, A. Alsaadi, Mathematical and numerical analysis of a fractional SIQR epidemic model with normalized Caputo–Fabrizio operator and machine learning approaches, *AIMS Math.*, **10** (2025), 20235–20261. https://doi.org/10.3934/math.2025904
17. J. Kim, Influence of fractional order on the behavior of a normalized time-fractional SIR model, *Mathematics*, **12** (2024), 3081. https://doi.org/10.3390/math12193081
18. A. Al-Quran, R. Shafqat, A. Alsaadi, A. M. Djaouti, Poliomyelitis dynamics with fractional order derivatives and deep neural networks, *Sci. Rep.*, **15** (2025), 32023. https://doi.org/10.1038/s41598-025-15195-2
19. J. Kim, A normalized Caputo–Fabrizio fractional diffusion equation, *AIMS Math.*, **10** (2025), 6195–6208. https://doi.org/10.3934/math.2025282
20. M. Jornet, Theory on new fractional operators using normalization and probability tools, *Fractal Fract.*, **8** (2024), 665. https://doi.org/10.3390/fractalfract8110665

AIMS Press